

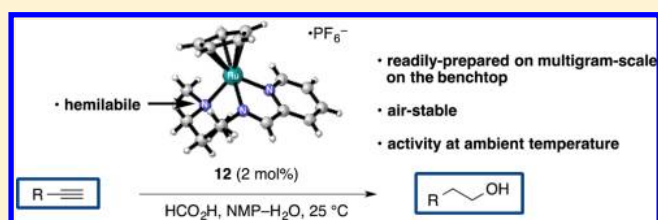
A Highly Active and Air-Stable Ruthenium Complex for the Ambient Temperature Anti-Markovnikov Reductive Hydration of Terminal Alkynes

Mingshuo Zeng, Le Li, and Seth B. Herzon*

Department of Chemistry, Yale University, New Haven, Connecticut 06520, United States

S Supporting Information

ABSTRACT: The conversion of terminal alkynes to functionalized products by the direct addition of heteroatom-based nucleophiles is an important aim in catalysis. We report the design, synthesis, and mechanistic studies of the half-sandwich ruthenium complex **12**, which is a highly active catalyst for the anti-Markovnikov reductive hydration of alkynes. The key design element of **12** involves a tridentate nitrogen-based ligand that contains a hemilabile 3-(dimethylamino)propyl substituent. Under neutral conditions, the dimethylamino substituent coordinates to the ruthenium center to generate an air-stable, 18-electron, κ^3 -complex. Mechanistic studies show that the dimethylamino substituent is partially dissociated from the ruthenium center (by protonation) in the reaction media, thereby generating a vacant coordination site for catalysis. These studies also show that this substituent increases hydrogenation activity by promoting activation of the reductant. At least three catalytic cycles, involving the decarboxylation of formic acid, hydration of the alkyne, and hydrogenation of the intermediate aldehyde, operate concurrently in reactions mediated by **12**. A wide array of terminal alkynes are efficiently processed to linear alcohols using as little as 2 mol % of **12** at ambient temperature, and the complex **12** is stable for at least two weeks under air. The studies outlined herein establish **12** as the most active and practical catalyst for anti-Markovnikov reductive hydration discovered to date, define the structural parameters of **12** underlying its activity and stability, and delineate design strategies for synthesis of other multifunctional catalysts.



INTRODUCTION

Linear alcohols are used throughout the commodity and fine chemical industries and this large demand renders the production of alcohols from hydrocarbon feedstocks an important goal in catalysis.¹ We have focused on developing methods to form linear alcohols from alkynes by anti-Markovnikov reductive hydration (Figure 1A). Such reactions have the potential to replace stoichiometric pathways, such as hydroboration–oxidation–reduction, which are mainstays of synthetic chemistry. Related and contemporaneous efforts to convert unsaturated hydrocarbons to linear alcohols have focused primarily on terminal alkenes and comprise the dual-catalytic anti-Markovnikov hydration of styrenes,² photoredox approaches to alkene hydroacyloxylation and hydroalkoxylation,³ hydroformylation–reduction,⁴ metal-catalyzed transfer hydrogenation–carbonyl addition,⁵ and allylic oxidation–hydrogenation.⁶

In the reductive hydration reaction we have developed, the alkyne is converted to an aldehyde by anti-Markovnikov hydration, and the aldehyde is reduced in situ to provide the alcohol (Figure 1A). We first reported a tandem two-catalyst system⁷ that employed the highly efficient hydration catalyst acetonitrile bis(2-diphenylphosphino-6-*t*-butylpyridine) (η^5 -cyclopentadienyl)ruthenium hexafluorophosphate, developed by Grotjahn and co-workers,⁸ and Shvo's catalyst⁹ to reduce the aldehyde intermediate (using 2-propanol as reductant). By utilizing a cationic gold–*N*-heterocyclic carbene complex¹⁰

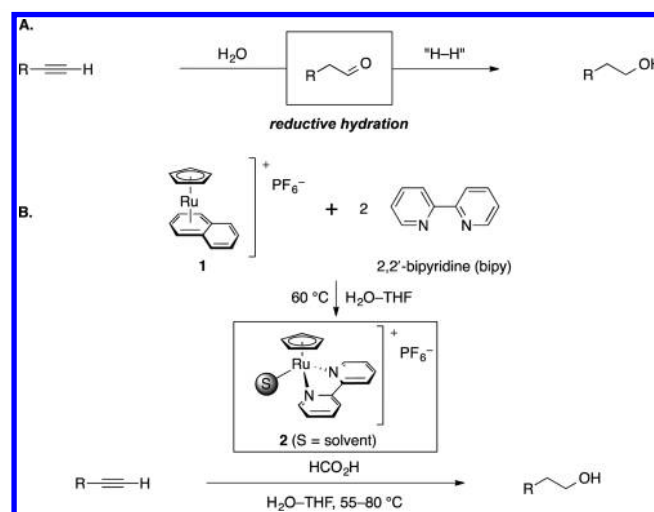


Figure 1. (A) Anti-Markovnikov reductive hydration. (B) Presumed active catalyst **2** in the anti-Markovnikov reductive hydration mediated by **1** and 2,2'-bipyridine (bipy).

in place of Grotjahn's catalyst, branched alcohols were also accessible.⁷

Received: February 24, 2014

Published: April 4, 2014

We recently reported that a single catalyst can support both the hydration and hydrogenation activities. A complex formed in situ from (η^5 -cyclopentadienyl)(η^6 -naphthalene)ruthenium hexafluorophosphate (**1**) and 2,2'-bipyridine (bipy) transforms terminal alkynes to linear alcohols in aqueous tetrahydrofuran using formic acid as reductant (Figure 1B).¹¹ In this system, preheating a mixture of the precursor **1** and an excess of bipy was necessary to generate the active catalyst. Preparative-scale experiments and X-ray crystallographic analysis suggested generation of structure **2**, in which the half-sandwich ruthenium fragment is ligated by bipy and a labile solvent molecule (S; acetonitrile in the X-ray analysis). A time-course analysis revealed that the hydration and hydrogenation activities of the catalyst were temporally separated, an effect we attributed to the production of stable catalyst–alkyne intermediates. As a consequence of its coordination environment, the complex **2** is air-sensitive and is difficult to isolate in pure form. Although this catalyst efficiently promoted the hydration step, the hydrogenation activity was modest, and elevated temperatures were required to achieve useful rates of reduction.

We have continued mechanistic studies of this reaction, with the goal of improving the catalyst activity, scope, and utility of the transformation. Herein we report the full evolution of our catalyst design studies, which have culminated in the identification of an air-stable, single-component catalyst that promotes the anti-Markovnikov reductive hydration at ambient temperature. This catalyst contains a hemilabile 3-(dimethylamino)propyl substituent that creates an 18-electron κ^3 -structure, rendering it amenable to use on a benchtop. Mechanistic studies show that the 3-(dimethylamino)propyl substituent partially dissociates under the reaction conditions to facilitate catalysis and that this functional group also increases hydrogenation activity. These studies also reveal a complex competition between at least three catalytic cycles involving the decarboxylation of the formic acid, alkyne hydration, and aldehyde hydrogenation.

■ CATALYST DESIGN, SYNTHESIS, AND ACTIVITY

In accord with literature reports,¹² we attributed the air-sensitivity of **2** to the presence of a labile monodentate ligand. To address this, we targeted for synthesis a hemilabile¹³ complex that could interconvert between a coordinatively saturated κ^3 -isomer and a reactive unsaturated κ^2 -isomer (Figure 2). We reasoned that the 18-electron κ^3 -state should be stable toward oxidative decomposition pathways. Upon activation and isomerization to κ^2 -binding, an open coordination site is generated, allowing catalysis to proceed. On the basis of studies of related half-sandwich ruthenium hydride complexes,¹⁴ it seemed likely that a monohydride [e.g., CpRu(bipy)H] is the active reducing agent in reactions catalyzed by **2**. We posited that a basic hemilabile functional group, such as an amine (X in Figure 2), could promote formation of these monohydride intermediates by mediating heterolytic cleavage of the reductant.¹⁵

Our studies focused on iminopyridine derivatives due to the modular nature of their synthesis and their similarity to bipy.¹⁶

Condensation of pyridine 2-carboxaldehyde with various amines formed the ligands **4–8** in 84–94% yield (Table 1). These ligands were conveniently associated with ruthenium by stirring with (η^5 -cyclopentadienyl)tris(acetonitrile)ruthenium hexafluorophosphate (**3**) in methylene chloride-*d*₂ at 25 °C. ¹H NMR analysis revealed nearly quantitative conversion to the iminopyridine complexes for all ligands except **5**.

By comparing the chemical shifts of the hydrogen atoms closest to the terminal functional group (H_a and H_b in **4–8**) in the free ligand and the complex, and the detection of coordinated acetonitrile, the mode of binding could be inferred.¹⁷ Thus, the 3-(methoxy)propylimine ligand **4** coordinated to ruthenium in the κ^2 -mode, providing the complex **9** ($\Delta\delta H_a, H_b, H_c = 0.04, 0.02, -0.02$, respectively; $\delta CH_3CN = 2.13$), whereas the alkynylimine ligand **6** formed the κ^3 -complex **10** ($\Delta\delta H_a, H_b, H_c = 1.87, 0.85, 0.43$, respectively). Observation of a nominal change in H_a and H_b chemical shifts ($\Delta\delta H_a, H_b, H_c = 0.03, 0.22, 0.32$, respectively) and the detection of bound acetonitrile ($\delta 2.13$) in the complex formed from the 2-(dimethylamino)-ethyl imine ligand **7** suggested generation of the κ^2 -structure **11**. On the other hand, the 3-(dimethylamino)propylimine **8** provided the κ^3 -complex **12**, as evidenced by a large shift in ligand resonances ($\Delta\delta H_a, H_b, H_c = -0.92, 0.98, 0.18$, and 1.06, respectively) and the absence of coordinated acetonitrile (see Supporting Information for additional spectroscopic data).

The structure of the complex **12** was confirmed by X-ray crystallography (Figure 3). The catalyst adopts a piano stool geometry, which is typical of cationic, half-sandwich ruthenium complexes.¹⁸ The dimethylamino–ruthenium (N-3–Ru) bond length in **12** is 2.227(2) Å, whereas the pyridine–ruthenium (N-1–Ru) and the imine–ruthenium bonds (N-2–Ru) are substantially shorter [2.083(3) and 2.048(2) Å, respectively]. The κ^3 binding mode may be favored by adoption of a well-defined chairlike geometry, as evidenced by the X-ray analysis and analysis of vicinal ¹H coupling constants.

The carbonyl complexes **13** and **14** were prepared to compare the electronic nature of the iminopyridine and bipyridine ligands (Table 2). The bipyridine complex **13** (1962 cm^{−1})^{18b} possesses a carbonyl stretch that is comparable to the iminopyridine complex **14** (1972 cm^{−1}), indicating that the two ligands possess similar electronic properties.

To benchmark the efficiencies of these catalysts, the reductive hydration of phenylacetylene (**15a**) was studied using 4.5 mol % of **2**, **10**, or **12** and 4.0 equiv of formic acid in aqueous *N*-methyl-2-pyrrolidinone (NMP) at 25 °C (Table 3).¹⁹ Under these conditions, the catalyst **2** efficiently converted **15a** to phenylacetaldehyde (**16a**), but consistent with the modest hydrogenation activity of the complex, none of the reduction product 2-phenethanol (**17a**) was detected (entry 1). We hypothesized that the alkyne function of the κ^3 -complex **10** may undergo conversion to an aldehyde or terminal alcohol, allowing catalysis, but this complex did not display activity (entry 2). This may reflect unfavorable geometries in the intramolecular functionalization of the alkyne. The κ^3 -complex **12**, however, was

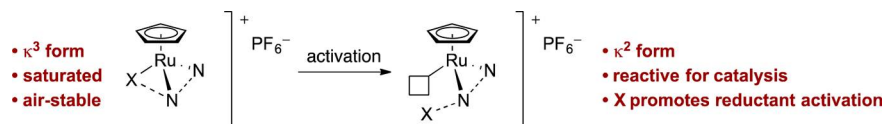


Figure 2. Catalyst design strategy.

Table 1. Syntheses and Structures of Complexes Derived from $[\text{CpRu}(\text{CH}_3\text{CN})_3]\text{PF}_6$ (3) and the Iminopyridine Ligands 4–8^a

ligand (4–8)	¹ H NMR shifts (δ)	complex (9–12)	¹ H NMR shifts (δ)
 4	H _a : 3.31, H _b : 3.45	 9	H _a : 3.35 H _b : 3.47, 3.43 CH ₃ CN: 2.13
 5	—	complex mixture	—
 6	H _a : 2.01, H _b : 2.30	 10	H _a : 3.88 H _b : 3.15, 2.73 CH ₃ CN: n/d ^b
 7	H _a : 2.25, H _b : 2.61	 11	H _a : 2.28 H _b : 2.83, 2.93 CH ₃ CN: 2.13
 8	H _a : 2.19, H _b : 2.32	 12	H _a : 1.27, 3.17 H _b : 2.50, 3.38 CH ₃ CN: n/d ^b

^aThe structures of the complexes 9–12 were elucidated by ¹H NMR spectroscopy of the unpurified product mixtures in methylene chloride-*d*₂. See Supporting Information for full spectroscopic data. ^bn/d = not detected.

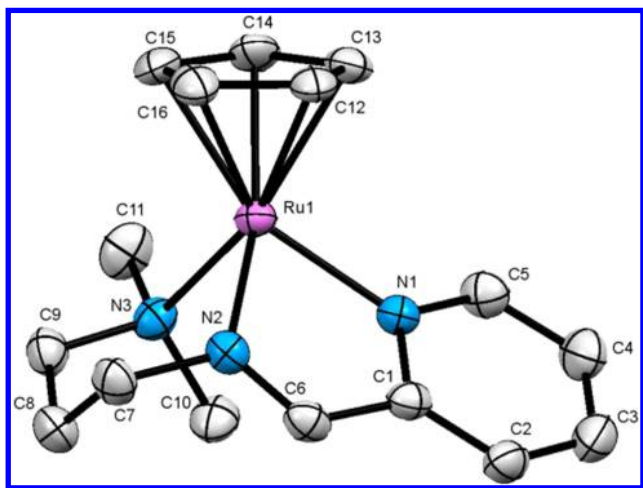


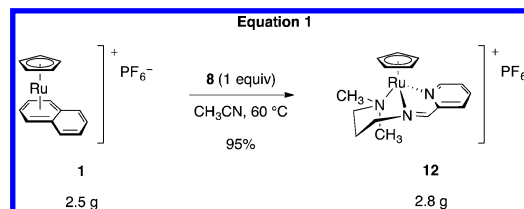
Figure 3. Molecular structure of the κ^3 -complex 12 (50% probability level). Hydrogen atoms and counterion are omitted for clarity.

Table 2. IR Stretching Frequencies of the Ruthenium Carbonyl Complexes 13 and 14

complex	ν_{CO} (cm ⁻¹)
 13	1962
 14	1972

remarkably active, and 4.5 mol % of 12 afforded a 98% yield of 17a after 24 h at 25 °C (entry 3). The yield of product was unchanged after storing the catalyst under air in a desiccator for two weeks (entry 4).

Given the superior activity of the complex 12, a preparative-scale synthesis was developed. Thus, stirring an equimolar mixture of the ligand 8 and the commercially available, air-stable ruthenium precursor 1 in acetonitrile at 60 °C formed 12 (eq 1). The product was isolated in 95% yield and >95% analytical purity (¹H NMR analysis) by extraction of the acetonitrile layer with reagent-grade hexanes (in a separatory funnel, open to air) and concentration. The complex 12 is stable for at least 2 weeks under air (vide supra) and can be stored in a vial under an inert gas (argon or nitrogen) indefinitely. Complex 12 will soon be available from Aldrich.

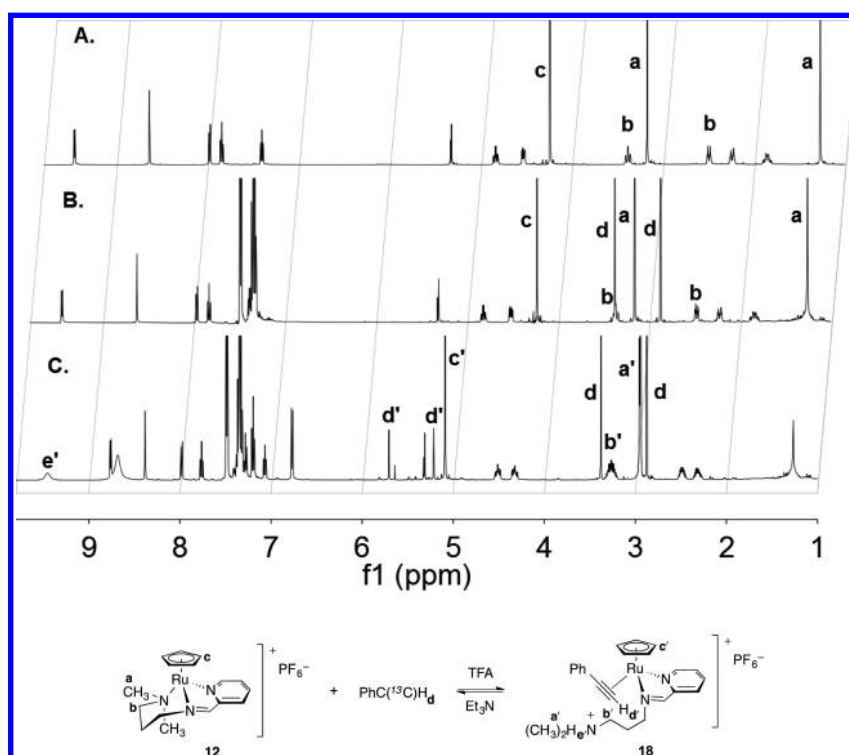


■ CATALYST ACTIVATION

Studies were conducted to probe the mechanism of the reductive hydration mediated by 12 and to determine the origins of its superior activity. A partially annotated ¹H NMR spectrum of 12 in methylene chloride-*d*₂ is shown in Figure 4A. Upon addition of

Table 3. Comparative Analysis of the Reductive Hydration Activity of 2, 10, and 12^a

$ \begin{array}{c} \text{Ph-C}\equiv\text{CH} \xrightarrow[\text{NMP-H}_2\text{O (0.3 M), 25 }^\circ\text{C}]{[\text{Ru}] (4.5 \text{ mol}\%), \text{HCO}_2\text{H (4.0 equiv)}} \text{Ph-CH=O} + \text{Ph-CH}_2\text{OH} \\ \text{15a} \qquad \qquad \qquad \text{16a} \qquad \qquad \qquad \text{17a} \end{array} $				
entry	[Ru]	15a	yield ^b 16a	17a
1 ^c		<1% ^d	>99%	<1% ^d
2		>99%	<1% ^d	<1% ^d
3		<1% ^d	<1% ^d	98%
4 ^e		<1% ^d	<1% ^d	98%

^aReaction conditions: 15a (150 μmol), 10 or 12 (6.75 μmol), formic acid (600 μmol), NMP-H₂O (4:1 v/v, [15a]₀ = 0.3 M), 25 °C, 24 h.^bDetermined by ¹H NMR spectroscopy using mesitylene as an internal standard. ^cCatalyst prepared in situ from 3 (6.75 μmol) and bipy (6.75 μmol). ^dNone was detected under conditions where 1% could be observed. ^eEmploying 12 after storage under air for two weeks in a desiccator.**Figure 4.** (A) ¹H NMR spectra of 12. (B) ¹H NMR spectra of 12 and [2-¹³C]phenylacetylene (5 equiv). (C) ¹H NMR spectra of 12, [2-¹³C]phenylacetylene (5 equiv), and trifluoroacetic acid (4 equiv). Spectra were recorded in methylene chloride-*d*₂ at 25 °C.

[2-¹³C]phenylacetylene (5 equiv), the resonances corresponding to 12 were essentially unchanged (Figure 4B). Addition of trifluoroacetic acid (4 equiv) resulted in formation of a new

complex in 95% yield (Figure 4C). We identified this species as the η²-alkyne complex 18. The alkyne C–H (H_{d'}) was observed as a doublet centered at δ 5.46 (¹J_{C–H} = 246 Hz), downfield of

free $[2-^{13}\text{C}]$ phenylacetylene (H_d , doublet, δ 3.12, $^1J_{\text{C-H}} = 251$ Hz). The free and coordinated terminal acetylene carbon atoms were observed at 137.2 and 122.9, respectively (^{13}C NMR and HMQC analysis). In addition, the iminopyridine chemical shifts of **12** and **18** are distinct. The methylene protons adjacent to the dimethylamino substituent (H_b) were observed at δ 2.50 and δ 3.38 in the κ^3 -complex **12**, and coalesced into one peak centered at δ 3.27 in **18** (H_b'). The methyl substituents of **12** (H_a) were well-resolved at δ 1.27 and δ 3.17, and coalesced into two partially overlapping doublets centered at δ 2.95 in the η^2 -alkyne complex **18** (H_a'). A COSY correlation was observed between the putative ammonium proton (H_e' , δ 9.45, br singlet) and H_a' and H_b' in the complex **18**. Addition of triethylamine (4 equiv) led to regeneration of **12** (18%) along with unidentified decomposition products. These results demonstrate that acidic conditions are needed to promote coordination of the alkyne.

To probe for this equilibrium in a setting relevant to catalysis, a related study was conducted in a mixture of *N,N*-dimethylformamide- d_7 - D_2O and in the presence of formic acid (Figure 5A, B).

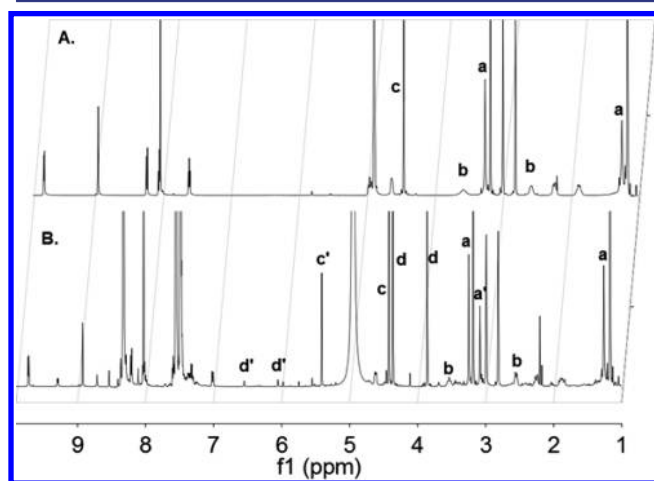


Figure 5. (A) ^1H NMR spectrum of **12** in *N,N*-dimethylformamide- d_7 - D_2O (4:1, v/v) at 0 °C. (B) ^1H NMR spectrum of **12**, $[2-^{13}\text{C}]$ -phenylacetylene (6.7 equiv), and formic acid (10.5 equiv), in *N,N*-dimethylformamide- d_7 - D_2O (4:1, v/v) at 0 °C, immediately after mixing. See Figure 4 for resonance assignments.

An NMR spectrum acquired immediately after mixing at 0 °C revealed formation of **18** in 20% yield, and the remainder of the ruthenium-containing complexes were accounted for by **12** (Figure 5B). Consistent with a reversible equilibrium between **12** and **18**, we observed a gradual decrease in the concentration of **12** as the reaction was warmed to ambient temperature and the $[2-^{13}\text{C}]$ phenylacetylene was consumed.

MECHANISTIC STUDIES

The reductive hydration of (2-fluorophenyl)acetylene (**19**, eq 2) was monitored by ^{19}F NMR spectroscopy at 10 min intervals (Figure 6). Temporal separation of the hydration and hydrogenation activities¹¹ was not observed, likely because the formation of catalyst–substrate complexes is incomplete using **12** (Figure 5). This behavior complicates a kinetics analysis because the rate of hydrogenation is coupled to the rate of hydration. Accordingly, we investigated each step separately to gain insights into the behavior of the catalyst.

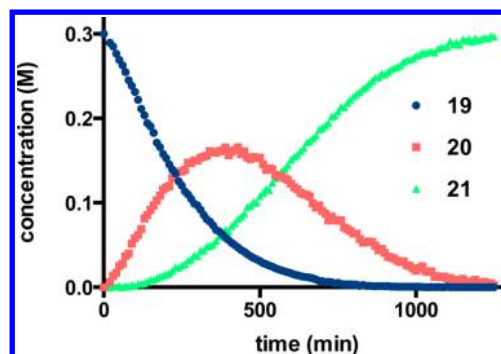
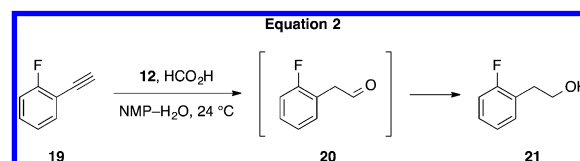


Figure 6. Reaction progress profile for the reductive hydration of (2-fluorophenyl)acetylene (**19**). Conditions: $[\textbf{19}]_0 = 0.300$ M, $[\textbf{12}]_0 = 0.0135$ M, $[\text{H}_2\text{O}]_0 = 11.1$ M, $[\text{HCO}_2\text{H}]_0 = 1.20$ M, NMP– H_2O (4:1 v/v), 23 °C.



To obtain information about the hydration step, we monitored the disappearance of (2-fluorophenyl)acetylene (**19**) and analyzed these data by reaction progress kinetic analysis.²⁰ The instantaneous rate of alkyne consumption was obtained from differentiation of plots of the fraction conversion of **19** versus

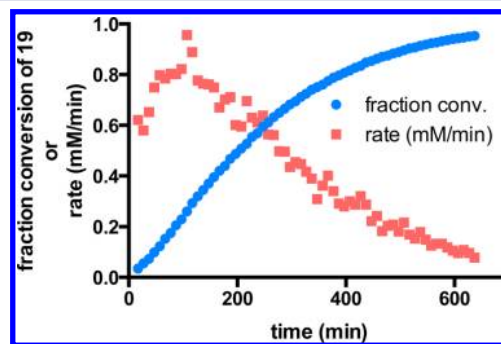


Figure 7. Reaction progress profile for the reductive hydration of (2-fluorophenyl)acetylene (**19**) monitored by ^{19}F NMR spectroscopy. Blue series: fraction conversion of **19** versus time. Red series: instantaneous rate versus time. Conditions: $[\textbf{19}]_0 = 0.300$ M, $[\textbf{12}]_0 = 0.0135$ M, $[\text{H}_2\text{O}]_0 = 11.1$ M, $[\text{HCO}_2\text{H}]_0 = 1.20$ M, NMP– H_2O (4:1 v/v), 23 °C.

time (Figure 7). Plots of the instantaneous rate versus time (red series in Figure 7) indicate that the rate gradually increases before decreasing in the manner expected for a reaction exhibiting positive-order kinetics in substrate. The observed induction period prevents analysis by the method of initial rates.

To establish the order in catalyst, two reactions were carried out using the same initial concentration of (2-fluorophenyl)acetylene (**19**), water, and formic acid, but with varying initial concentrations of **12** (13.5 and 20.4 mM). Plots of $\text{rate}/[\textbf{12}]_0$ versus $[\textbf{19}]$ overlaid, establishing the hydration as first order in **12** (Figure 8).

Figure 9 shows that the relationship between reaction rate and formic acid equivalents is complex. The rate of reaction at $[\text{HCO}_2\text{H}]_0 = 0.600$ or 1.50 M (2.0 and 5.0 equiv with respect to **19**, green and orange curves, respectively) is less than that at

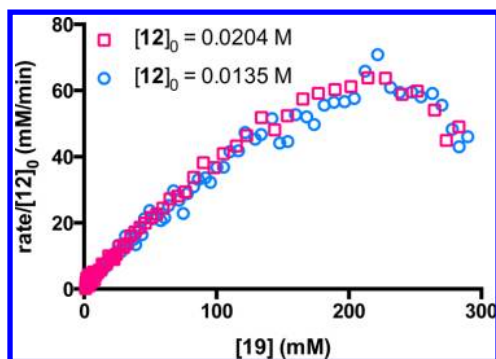


Figure 8. A. Plot of $\text{rate}/[\mathbf{12}]_0$ versus $[\mathbf{19}]$ reveals a first order dependence on $\mathbf{12}$. Conditions: $[\mathbf{19}]_0 = 0.300$ M, $[\mathbf{12}]_0 = 0.0135$ or 0.0204 M, $[\text{H}_2\text{O}]_0 = 11.1$ M, $[\text{HCO}_2\text{H}]_0 = 1.20$ M, NMP– H_2O (4:1 v/v), 23°C .

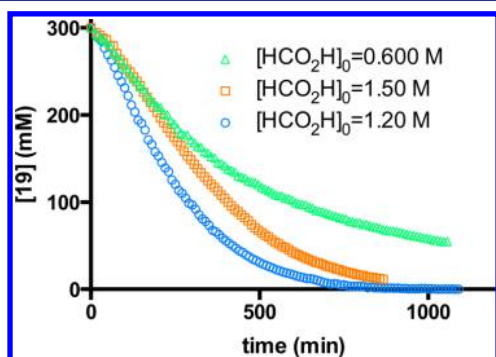


Figure 9. Plot $[\mathbf{19}]$ versus time at varying initial concentrations of formic acid. Conditions: $[\mathbf{19}]_0 = 0.300$ M, $[\text{H}_2\text{O}]_0 = 11.1$ M, $[\mathbf{12}]_0 = 0.0135$ M, NMP– H_2O (4:1 v/v), 23°C .

$[\text{HCO}_2\text{H}]_0 = 1.20$ M (4.0 equiv with respect to $\mathbf{19}$, blue curve), and the reaction beginning with $[\text{HCO}_2\text{H}]_0 = 0.6$ M does not proceed to completion. The slower rate at a higher concentration of formic acid is attributed to inhibition of the hydration step by partitioning of the catalyst toward a nonproductive, decarboxylation pathway (see below). At lower concentrations of formic acid, the slower rate may arise from gradual neutralization of the reaction media by this decarboxylation pathway and deactivation of the catalyst by formation of the κ^3 -isomer.

Figure 10 shows $[\mathbf{19}]$ versus time in a pair of “same excess” experiments, which are frequently used to probe for catalyst

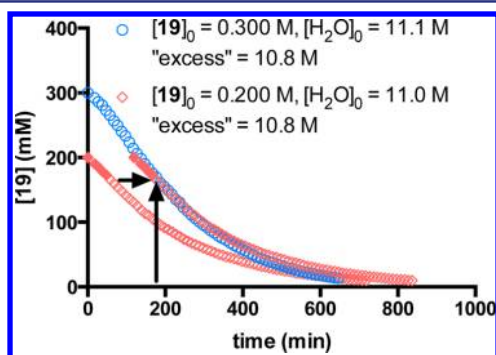
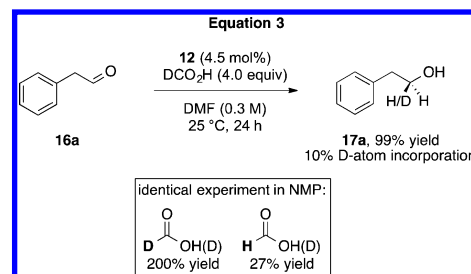


Figure 10. Plot of $[\mathbf{19}]$ versus time in a pair of “same-excess” experiments; the experiments have different values of $[\mathbf{19}]_0$ and $[\text{H}_2\text{O}]_0$, with the difference between the two (defined as the “excess” = $[\mathbf{19}]_0 - [\text{H}_2\text{O}]_0$) held the same. Common conditions: $[\mathbf{12}]_0 = 0.0135$ M, $[\text{HCO}_2\text{H}]_0 = 1.20$ M, NMP– H_2O (4:1 v/v), 23°C . Solid red points denote the induction period.

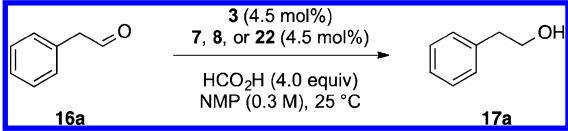
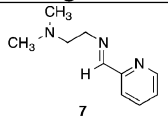
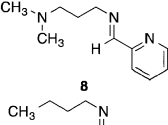
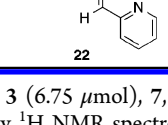
deactivation or product inhibition.²⁰ To remove complications arising from the induction period, we disregard the early data points in the red series (indicated by the solid red points) from the analysis. The concentrations of (2-fluorophenyl)acetylene ($\mathbf{19}$) and water in both runs are identical at the time point indicated by the arrows in the figure. By shifting the first time point of the red series to overlay with the blue series, the rates of these two reactions can be compared. In a normal time-adjusted plot, the experiment with a higher concentration of starting material is typically as fast as or slower than that beginning with a lower concentration of starting material, and a slower rate is an indication of product inhibition or catalyst deactivation.²⁰ As is apparent from this analysis, the time-adjusted plots diverge and the experiment starting from a higher concentration of $\mathbf{19}$ (blue series) displays a faster rate than that beginning from a lower concentration of $\mathbf{19}$ (red series). The faster rate for the reaction starting from a higher concentration of $\mathbf{19}$ may arise from a decrease in the ratio of formic acid to $\mathbf{19}$, which shifts the distribution of catalyst toward the hydration cycle (see Figure 11 below). However, this increase in rate may mask smaller effects arising from product inhibition or catalyst decomposition.

To gain insight into the reduction step,²¹ we studied the hydrogenation of phenylacetaldehyde ($\mathbf{16a}$) using DCO_2H as reductant (eq 3). The experiment was conducted in DMF to avoid the potential for H/D exchange with NMP. The reduction proceeded in nearly quantitative yield and with 10% deuterium atom incorporation at the carbinol center of $\mathbf{17a}$, as determined by ^1H and ^2H NMR analysis. This result suggests loss of the identity of the formyl hydrogen (deuterium) and oxygen hydrogen atoms by decarboxylation of formic acid²² and formation of HD. Reduction may occur via a ruthenium hydride, and the selective incorporation of hydrogen into the aldehyde may reflect primary and equilibrium kinetic isotope effects for formation of the ruthenium hydride and addition to the carbonyl.^{14d} Repeating the experiment in NMP allowed for quantification of the formic acid isotopologs at the end of the experiment. In this experiment, we obtained a 200% yield of $\text{DCO}_2(\text{H/D})$ (theoretical: 300%) and a 27% yield of $\text{HCO}_2(\text{H/D})$. The most reasonable explanation for production of $\text{HCO}_2(\text{H/D})$ involves exchange of the deuterium and proton positions by reduction of carbon dioxide with HD (e.g., reversal of the decarboxylation pathway).



This latter result suggested that a ruthenium hydride may be accessible from $\mathbf{12}$ and dihydrogen. To test this, we monitored the reduction of phenylacetaldehyde ($\mathbf{16a}$) using dihydrogen (introduced by bubbling dihydrogen through the reaction solution for 1 min), catalyst $\mathbf{12}$, and trifluoroacetic acid (TFA, 1 equiv with respect to ruthenium) as activator (eq 4). Under these conditions, 2-phenethanol ($\mathbf{17a}$) was formed in 30% yield, with the remainder of material in this experiment accounted for as unreacted $\mathbf{16a}$. The difference in yields of $\mathbf{17a}$ using dihydrogen and formic acid may arise from variations in the acidity of the reaction media and the low pressure of dihydrogen

Table 4. Reduction of Phenylacetaldehyde (16a) Using Complexes Formed In Situ from Ligand 7, 8, or 22 and the Precursor 3^a

				
entry	ligand	16a	yield ^b 17a	HCO ₂ H ^c
1		<1%	99%	2%
2		<1%	99%	98%
3		90%	9%	280%

^aReaction conditions: 16a (150 μ mol), 3 (6.75 μ mol), 7, 8, or 22 (6.75 μ mol), formic acid (600 μ mol), NMP–H₂O (4:1 v/v, 500 μ L, [16a]₀ = 0.300 M), 25 °C, 24 h. ^bDetermined by ¹H NMR spectroscopy using mesitylene as an internal standard. ^cYield of formic acid based on starting material.

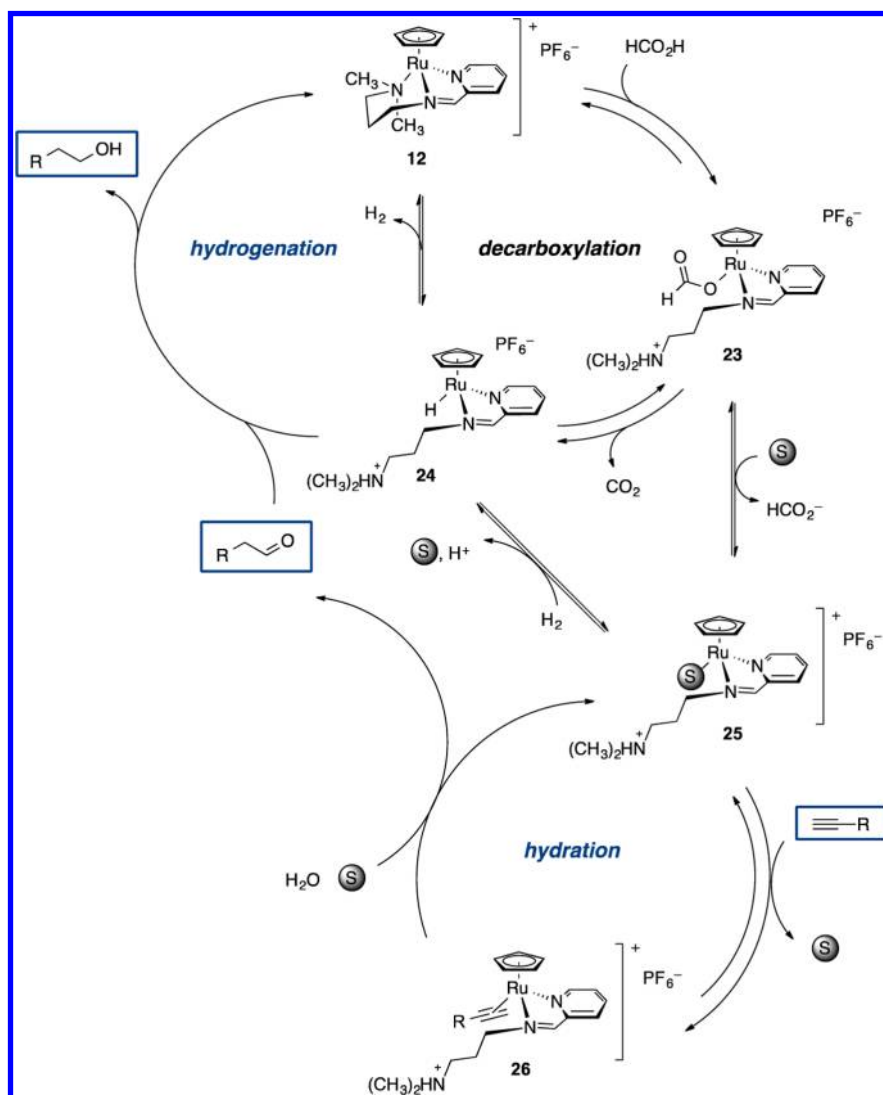
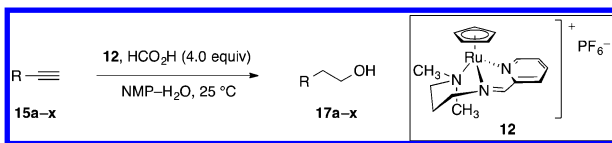
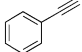
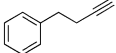
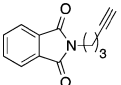
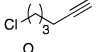
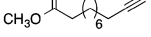
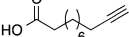
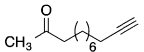
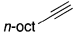
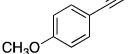
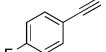
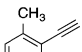
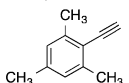
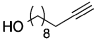
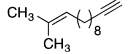
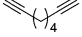
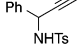
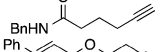
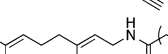
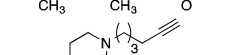
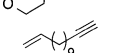
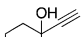
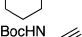
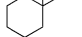
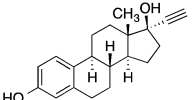


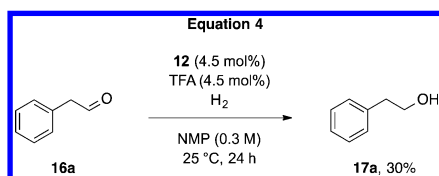
Figure 11. Proposed catalytic cycles that are operative during reductive hydration reactions mediated by 12.

Table 5. Substrate Scope for Reductive Hydration Employing Complex 12^a

entry	substrate	mol% Ru	yield ^b
1		2	83%
2		2	87%
3		2	94% (89%) ^c
4		2	92%
5		2	90%
6		2	89%
7 ^d		2	90%
8		2	94%
9		2	84%
10		2	83%
11		2	84%
12		9	92%
13		4.5	90%
14 ^e		4.5	88%
15		4.5	89%
16		4.5	93%
17		4.5	90%
18		4.5	91%
19		4.5	86%
20 ^e		4.5	64%
21 ^f		9	56%
22 ^f		9	69%
23 ^f		9	89%
24 ^g		9	45%

^aReactions were performed on a 500 μ mol scale at 25 $^{\circ}$ C in 4:1 (v/v) NMP–H₂O, for 48 h; [alkyne]₀ = 300 mM. ^bIsolated yield after purification by flash-column chromatography. ^cEmploying 1.28 g (6.00 mmol) of the alkyne **15c**. ^d60 h. ^e2.5 mol % of trifluoroacetic acid was added. ^f5 mol % of trifluoroacetic acid was added. ^g[**15x**]₀ = 204 mM, 8 mol % of trifluoroacetic acid was employed.

used in the experiment in eq 4.²³ In the absence of TFA, the reduction did not occur, in accord with our NMR studies above.



To test for a rate enhancement in the activation of formic acid arising from the dimethylamino substituent of **12**, we evaluated the reduction of phenylacetaldehyde (**16a**) by catalysts formed in situ from the acetonitrile precursor **3** and the ligands **7**, **8**, and **22** (Table 4). In these experiments, four equivalents of formic acid were employed. The complexes derived from the 2-(dimethylamino)ethyl ligand **7** and the 3-(dimethylamino)propyl ligand **8** efficiently reduced the starting material **16a** (entries 1 and 2). The complex derived from the *N*-butylimino ligand **22**, however, was less effective for the reduction (9% yield of **17a**, entry 3), even though it cannot access an unreactive κ^3 -form. In addition, we observed that nearly all of the formic acid was depleted in the reaction employing ligand **7** (entry 1), whereas only 75% of the formic acid employed was depleted in reactions employing **8** (entry 2). These experiments indicate that the decarboxylation of formic acid occurs at a rate that exceeds hydrogenation of **16a**.

MECHANISTIC MODEL

Based on the experiments presented above, we propose that three catalytic cycles are operating concurrently in reductive hydration reactions mediated by **12**. These include a hydration cycle, a decarboxylation cycle that interconverts formic acid with dihydrogen and carbon dioxide, and a hydrogenation cycle that reduces the aldehyde to an alcohol (Figure 11).

In the absence of acid, the catalyst exists in the κ^3 -form. Under the acidic conditions of the reductive hydration reaction, protonation, solvolysis, and substrate association occur, to lead to the η^2 -alkyne complex **26**. The complex **26** lies outside of the hydrogenation and decarboxylation cycles, and the observed induction period in the hydration step (Figure 7) can be explained by the partitioning of **12** between these cycles and the hydration cycle. At the initial stages of the reaction, a larger proportion of the catalyst is contained within the decarboxylation cycle, which leads to a slower initial rate of alkyne consumption. As the concentration of formic acid decreases, the distribution of catalyst shifts toward the hydration cycle, increasing the rate of consumption of alkyne. Significant decreases in the formic acid concentration induce catalyst deactivation by neutralization and formation of the κ^3 -isomer, leading to incomplete conversion of substrate (see Figure 9). The hydration step may proceed by addition of water to a metal vinylidene intermediate (derived from the η^2 -alkyne complex **26**), as has been proposed for ruthenium-based anti-Markovnikov alkyne hydration catalysts.^{8c–e,24}

Our studies of the hydrogenation step conclusively establish that the pendant amine accelerates the rate of reduction. The amine may serve as a proton shuttle, facilitating the formation of the ruthenium formate **23**, which may decarboxylate to generate the ruthenium hydride **24**.^{14d} Elimination of dihydrogen would regenerate **12**. The observed deuterium scrambling in reactions employing DCO₂H and the successful reduction of **16a** with dihydrogen indicate this pathway is reversible. Prior studies have established the activating role of pendant amines in the generation of ruthenium and iridium

hydride complexes from dihydrogen,²⁵ and the lower (9%) yield of reduction product employing the alkylimine ligand **22** (Table 4) is consistent with participation of the amine in the hydrogenation step. We postulate that reduction occurs via outer sphere delivery of hydride from **24**, potentially assisted by hydrogen bonding of the carbonyl oxygen to the ammonium ion.¹⁵

SUBSTRATE SCOPE

The scope and limitations of the catalyst **12** are shown in Table 5. For all of the substrates examined, the reductive hydration proceeded at ambient temperature, and for many substrates (entries 1–11), 2 mol % of **12** was sufficient to achieve complete conversion. Both aromatic and aliphatic alkynes (**15a–k**) gave high isolated yields at 2 mol % of catalyst loading. The catalyst and reaction conditions are compatible with many functional groups including phthalimides (**15c**), primary alkyl chlorides (**15d**), esters (**15e**), and carboxylic acids (**15f**). Substrates containing free alcohols (**15m**), di- or trisubstituted alkenes (**15n**, **15r**, **15s**), amides (**15q**, **15s**), and tertiary amines (**15t**) required 4.5 mol % of **12** to achieve full conversion. Of particular note, propargylic alcohols such as **15v** and **15x** are converted to product at ambient temperature (69 and 49% yield for **15v** and **15x**, respectively). Substrates such as **15v** do not provide high yields of product with earlier reductive hydration catalysts.¹¹ A reaction conducted on a 6 mmol scale proceeded in comparable yield to 500 μ mol scale (89% and 94% for 6 mmol and 500 μ mol scale, respectively; entry 3). A limitation of this catalyst can be observed with sterically-encumbered substrates such as **15l**. These substrates require higher catalyst loading (9 mol %) and additional trifluoroacetic acid to obtain high conversions. Presumably, the rates of hydration and/or hydrogenation are decreased due to unfavorable nonbonded interactions with the catalyst.

CONCLUSION

In summary, we have reported the design, synthesis, and mechanistic studies of a highly active catalyst for the anti-Markovnikov reductive hydration of alkynes. The catalyst builds on our preliminary studies of the bipy complex **2**. The catalyst **12** is easily prepared on a multigram scale, is stable for at least two weeks under air (and can be stored indefinitely under argon), and can be employed without recourse to a glovebox. Mechanistic studies suggest that the stability of the catalyst arises from coordination of a hemilabile amine to the ruthenium center. These studies also showed that the pendant amine increases the hydrogenation activity of the catalyst. These investigations revealed a complex interplay between hydration, hydrogenation, and decarboxylation cycles. The catalyst displays the highest activity of any reductive hydration system reported to date, allowing reactions to be conducted at ambient temperature for the first time. The mechanistic studies outlined herein will inform the development of other anti-Markovnikov reductive functionalization reactions.

ASSOCIATED CONTENT

Supporting Information

Detailed experimental procedures and characterization data for all new compounds. This material is available free of charge via the Internet at <http://pubs.acs.org>.

■ AUTHOR INFORMATION

Corresponding Author

seth.herzon@yale.edu

Notes

The authors declare no competing financial interest.

■ ACKNOWLEDGMENTS

Financial support from the David and Lucile Packard Foundation is gratefully acknowledged.

■ REFERENCES

- (1) Arpe, H.-J.; Weissmehl, K. *Industrial Organic Chemistry*; Wiley-VCH: Weinheim, 2010.
- (2) Dong, G. B.; Teo, P. L.; Wickens, Z. K.; Grubbs, R. H. *Science* **2011**, 333, 1609.
- (3) (a) Hamilton, D. S.; Nicewicz, D. A. *J. Am. Chem. Soc.* **2012**, 134, 18577. (b) Perkowski, A. J.; Nicewicz, D. A. *J. Am. Chem. Soc.* **2013**, 135, 10334.
- (4) (a) Chevallier, F.; Breit, B. *Angew. Chem., Int. Ed.* **2006**, 45, 1599. (b) Takahashi, K.; Yamashita, M.; Ichihara, T.; Nakano, K.; Nozaki, K. *Angew. Chem., Int. Ed.* **2010**, 49, 4488.
- (5) Smejkal, T.; Han, H.; Breit, B.; Krische, M. J. *J. Am. Chem. Soc.* **2009**, 131, 10366.
- (6) Campbell, A. N.; White, P. B.; Guzei, I. A.; Stahl, S. S. *J. Am. Chem. Soc.* **2010**, 132, 15116.
- (7) Li, L.; Herzon, S. B. *J. Am. Chem. Soc.* **2012**, 134, 17376.
- (8) (a) Grotjahn, D. B.; Incarvito, C. D.; Rheingold, A. L. *Angew. Chem., Int. Ed.* **2001**, 40, 3884. (b) Grotjahn, D. B.; Lev, D. A. *J. Am. Chem. Soc.* **2004**, 126, 12232. (c) Grotjahn, D. B.; Miranda-Soto, V.; Kragulj, E. J.; Lev, D. A.; Erdogan, G.; Zeng, X.; Cooksy, A. L. *J. Am. Chem. Soc.* **2007**, 130, 20. (d) Grotjahn, D. B.; Kragulj, E. J.; Zeinalipour-Yazdi, C. D.; Miranda-Soto, V.; Lev, D. A.; Cooksy, A. L. *J. Am. Chem. Soc.* **2008**, 130, 10860. For a review, see (e) Grotjahn, D. B. *Pure Appl. Chem.* **2010**, 82, 635.
- (9) (a) Blum, Y.; Shvo, Y. *Isr. J. Chem.* **1984**, 24, 144. (b) Shvo, Y.; Czarkie, D.; Rahamim, Y.; Chodosh, D. F. *J. Am. Chem. Soc.* **1986**, 108, 7400. For a review, see (c) Warner, M. C.; Casey, C. P.; Bäckvall, J.-E. *Top. Organomet. Chem.* **2011**, 37, 85.
- (10) Marion, N.; Ramón, R. S.; Nolan, S. P. *J. Am. Chem. Soc.* **2008**, 131, 448.
- (11) Li, L.; Herzon, S. B. *Nat. Chem.* **2014**, 6, 22.
- (12) (a) Palacios, M. D.; Puerta, M. C.; Valerga, P.; Lledós, A.; Veilly, E. *Inorg. Chem.* **2007**, 46, 6958. (b) Kim, K.; Kishima, T.; Matsumoto, T.; Nakai, H.; Ogo, S. *Organometallics* **2012**, 32, 79.
- (13) For a review of hemilabile ligands in catalysis, see Braunstein, P.; Naud, F. *Angew. Chem., Int. Ed.* **2001**, 40, 680.
- (14) For selected examples, see (a) Jia, G.; Morris, R. H. *J. Am. Chem. Soc.* **1991**, 113, 875. (b) Jia, G.; Lough, A. J.; Morris, R. H. *Organometallics* **1992**, 11, 161. (c) Magee, M. P.; Norton, J. R. *J. Am. Chem. Soc.* **2001**, 123, 1778. (d) Guan, H.; Iimura, M.; Magee, M. P.; Norton, J. R.; Zhu, G. *J. Am. Chem. Soc.* **2005**, 127, 7805. (e) Guan, H.; Saddoughi, S. A.; Shaw, A. P.; Norton, J. R. *Organometallics* **2005**, 24, 6358. (f) O, W. W. N.; Lough, A. J.; Morris, R. H. *Organometallics* **2012**, 31, 2137. (g) Silant'ev, G. A.; Filippov, O. A.; Tolstoy, P. M.; Belkova, N. V.; Epstein, L. M.; Weisz, K.; Shubina, E. S. *Inorg. Chem.* **2013**, 52, 1787.
- (15) For reviews of functional ligands in catalysis, see (a) Morris, R. H. *Chem. Soc. Rev.* **2009**, 38, 2282. (b) Crabtree, R. H. *New J. Chem.* **2011**, 35, 18. (c) Eisenstein, O.; Crabtree, R. H. *New J. Chem.* **2013**, 37, 21.
- (16) For a review of iminopyridine ligands, see Chelucci, G. *Coord. Chem. Rev.* **2013**, 257, 1887.
- (17) For examples of related approaches to ligand binding analysis, see (a) Tein-Fu, W.; Tsung-Yi, L.; Jim-Wen, C.; Chi-Wi, O. *J. Organomet. Chem.* **1992**, 423, 31. (b) Wang, T.-F.; Wen, Y.-S. *J. Organomet. Chem.* **1992**, 439, 155. (c) Flores, J. C.; Chien, J. C. W.; Rausch, M. D. *Organometallics* **1994**, 13, 4140. (d) van der Zeijden, A. A. H. *J. Organomet. Chem.* **1996**, 518, 147. (e) Wang, T.-F.; Lai, C.-Y.; Wen, Y.-S. *J. Organomet. Chem.* **1996**, 523, 187. (f) Philippopoulos, A. I.; Hadjiliadis, N.; Hart, C. E.; Donnadieu, B.; Mc Gowan, P. C.; Poilblanc, R. *Inorg. Chem.* **1997**, 36, 1842.
- (18) (a) Albers, M. O.; Liles, D. C.; Robinson, D. J.; Singleton, E. *Organometallics* **1987**, 6, 2179. (b) Balavoine, G. G. A.; Boyer, T.; Livage, C. *Organometallics* **1992**, 11, 456.
- (19) We have found that polar aprotic solvents such as *N*-methyl-2-pyrrolidinone or *N,N*-dimethylformamide are superior to tetrahydrofuran. Le Li and Seth B. Herzon, unpublished results.
- (20) (a) Blackmond, D. G. *Angew. Chem., Int. Ed.* **2005**, 44, 4302. (b) Mathew, J. S.; Klussmann, M.; Iwamura, H.; Valera, F.; Futran, A.; Emanuelsson, E. A. C.; Blackmond, D. G. *J. Org. Chem.* **2006**, 71, 4711.
- (21) For a review of metal-catalyzed transfer hydrogenation, see Samec, J. S. M.; Bäckvall, J.-E.; Andersson, P. G.; Brandt, P. *Chem. Soc. Rev.* **2006**, 35, 237.
- (22) For selected examples of transition metal-mediated decarboxylation of formic acid, see (a) Gao, Y.; Kuncheria, J. K.; Jenkins, H. A.; Puddephatt, R. J.; Yap, G. P. A. *J. Chem. Soc., Dalton Trans.* **2000**, 3212. (b) Junge, H.; Boddien, A.; Capitta, F.; Loges, B.; Noyes, J. R.; Gladiali, S.; Beller, M. *Tetrahedron Lett.* **2009**, 50, 1603. (c) Fukuzumi, S.; Kobayashi, T.; Suenobu, T. *J. Am. Chem. Soc.* **2010**, 132, 1496. (d) Majewski, A.; Morris, D. J.; Kendall, K.; Wills, M. *ChemSusChem* **2010**, 3, 431. (e) Boddien, A.; Gartner, F.; Federsel, C.; Sponholz, P.; Mellmann, D.; Jackstell, R.; Junge, H.; Beller, M. *Angew. Chem., Int. Ed.* **2011**, 50, 6411. (f) Boddien, A.; Mellmann, D.; Gartner, F.; Jackstell, R.; Junge, H.; Dyson, P. J.; Laurenczy, G.; Ludwig, R.; Beller, M. *Science* **2011**, 333, 1733. (g) Himeda, Y.; Miyazawa, S.; Hirose, T. *ChemSusChem* **2011**, 4, 487. (h) Papp, G.; Csorba, J.; Laurenczy, G.; Joo, F. *Angew. Chem., Int. Ed.* **2011**, 50, 10433. (i) Hull, J. F.; Himeda, Y.; Wang, W.-H.; Hashiguchi, B.; Periana, R.; Szalda, D. J.; Muckerman, J. T.; Fujita, E. *Nat. Chem.* **2012**, 4, 383. (j) Barnard, J. H.; Wang, C.; Berry, N. G.; Xiao, J. *Chem. Sci.* **2013**, 4, 1234.
- (23) Effervescence is observed upon venting reactions employing formic acid as reductant, suggesting the pressure of the vessel is higher than that of equation 4 (1 atm). This increase in pressure may increase the hydrogenation activity of the catalyst.
- (24) Tokunaga, M.; Suzuki, T.; Koga, N.; Fukushima, T.; Horiuchi, A.; Wakatsuki, Y. *J. Am. Chem. Soc.* **2001**, 123, 11917.
- (25) (a) Chu, H. S.; Lau, C. P.; Wong, K. Y.; Wong, W. T. *Organometallics* **1998**, 17, 2768. (b) Lee, D.-H.; P. Patel, B.; H. Crabtree, R.; Clot, E.; Eisenstein, O. *Chem. Commun.* **1999**, 297. (c) Gruet, K.; Crabtree, R. H.; Lee, D.-H.; Liable-Sands, L.; Rheingold, A. L. *Organometallics* **2000**, 19, 2228. (d) Gruet, K.; Clot, E.; Eisenstein, O.; Lee, D. H.; Patel, B.; Macchioni, A.; Crabtree, R. H. *New J. Chem.* **2003**, 27, 80. (e) DiMondo, D.; Thibault, M. E.; Britten, J.; Schlaf, M. *Organometallics* **2013**, 32, 6541.